Fejtova et al., http://www.jcb.org/cgi/content/full/jcb.200807155/DC1

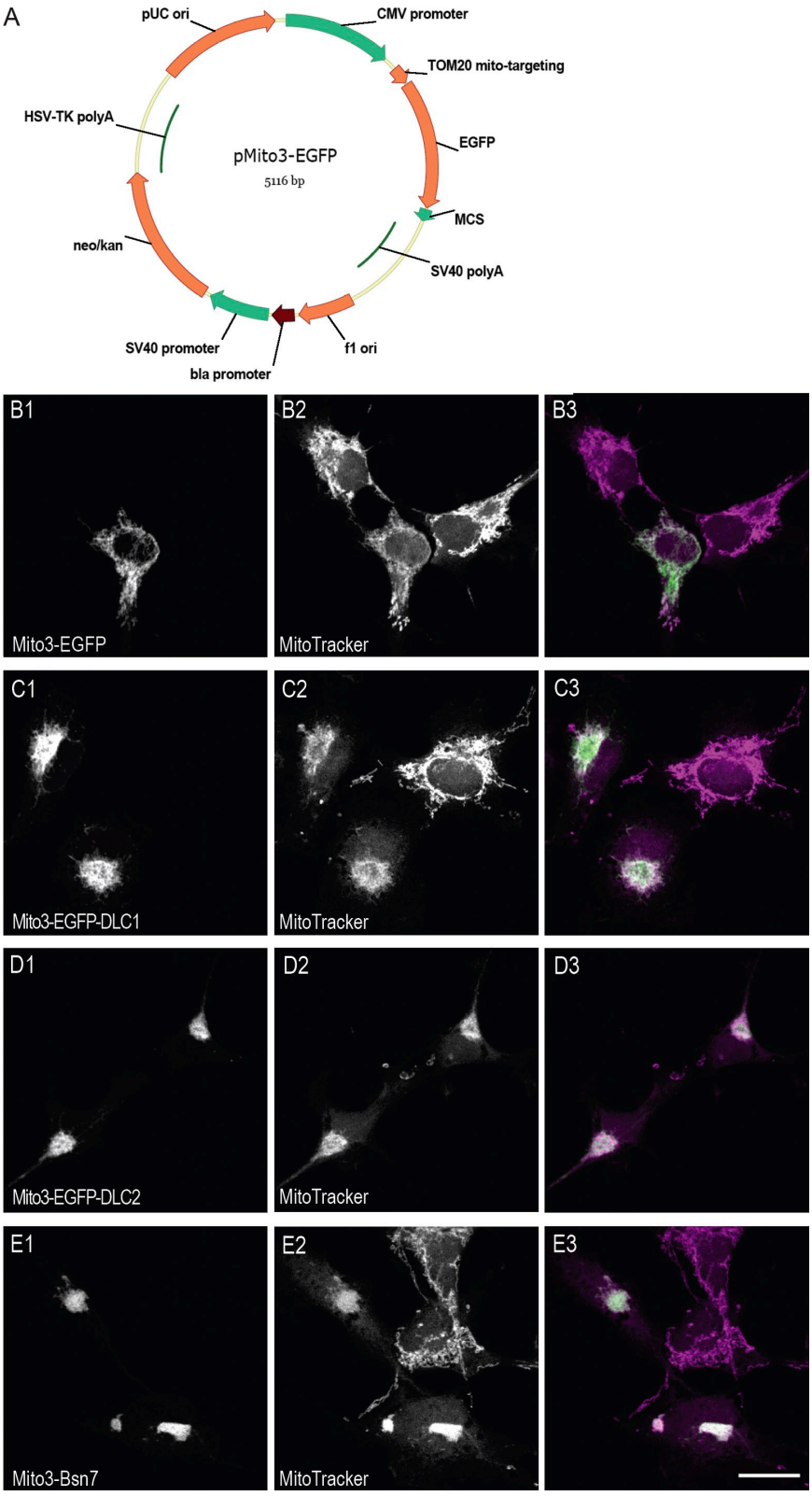


Figure S1. **Mitochondrial localization of fusion constructs using TOM20 mitochondrial targeting domain.** (A) Map of expression vector for mito-targeted EGFP. DLC1, DLC2, and Bassoon fragments were cloned in frame using the multiple cloning site (MCS). bla, β-lactamase; CMV, cytomegalovirus; HSV-TK, herpes simplex virus thymidine kinase; neo/kan, neomycin/kanamycin; ori, origin of replication. (B–E) Cells were transfected with mito-targeting constructs, and, 18 h after transfection, mitochondria were stained using MitoTracker before fixation of cells. Colocalization of GFP fluorescence (first and third column) with MitoTracker (second and third column) confirmed correct targeting of expressed Mito3-EGFP and its fusion proteins. Note the change in distribution of mitochondria after mito-targeting of EGFP (B1–B3) in contrast to mito-targeting of DLCs (C1–C3 and D1–D3) or Bsn7 fragment (E1–E3). Bar, 20 μm.

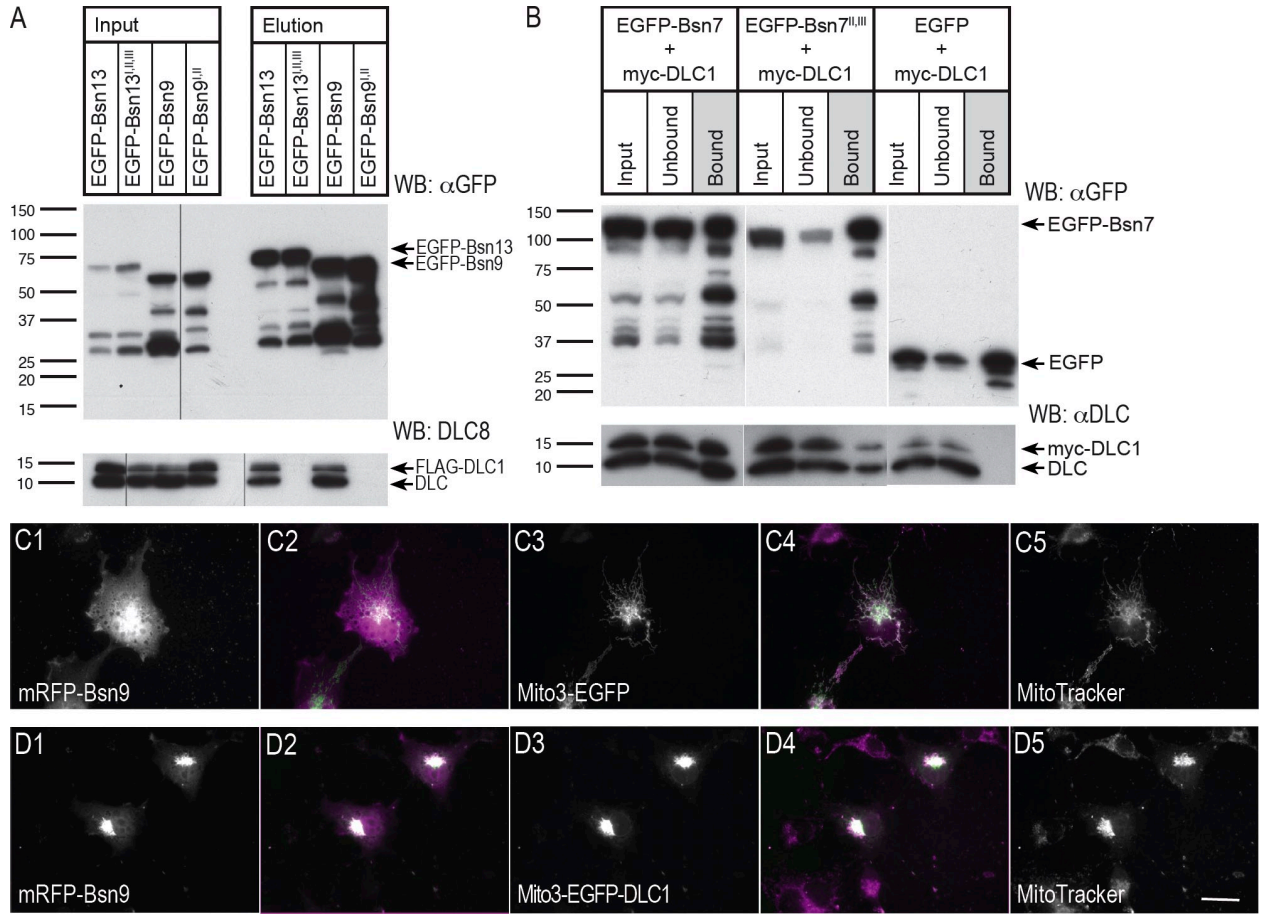


Figure S2. **Bassoon interacts with DLC1 and DLC2 in mammalian cells.** (A and B) Coimmunoprecipitation of Bassoon–DLC complexes from HEK293T cells. Lysates from transfected cells with EGFP-tagged Bsn9 and Bsn13 and the point-mutated constructs Bsn9$^{II,III}$ and Bsn13$^{I,II,III}$ (A) or with Bsn7, Bsn7$^{II,III}$, or EGFP (B) and Flag- (A) or myc-tagged (B) DLC1 were incubated with anti-GFP antibodies coupled to magnetic beads. The samples of input material (Input), unbound material (Unbound), and eluted material (Elution) were separated by SDS-PAGE and detected with antibodies against GFP (top), DLC8 antibody (A, bottom), or anti-DLC antibody (B, bottom) on WBs. All EGFP-tagged proteins and EGFP were expressed (I and Input lanes) and successfully immunoprecipitated (arrows in α-GFP WBs in A and B). Overexpressed DLC1 and endogenous DLCs were coimmunoprecipitated with EGFP-tagged Bsn9 and Bsn13 but not with the constructs carrying point mutations in their DLC-binding sites (A). EGFP-tagged Bsn7 coprecipitated overexpressed DLC1 and endogenous DLCs more efficiently than EGFP-Bsn7$^{II,III}$, which contains only one active DLC-binding site (site I), whereas sites II and III were mutated. DLC was not coprecipitated with EGFP. Black/white lines indicate that intervening lanes have been spliced out. Molecular mass is indicated in kilodaltons. (C and D) Mito-targeting assays in COS-7 cells of Bsn9 fragment. Cells were fixed 18 h after transfection. Mito-targeted EGFP or EGFP-DLC1 are localized at mitochondria (C3 and D3; green in overlay images), as shown by colocalization with MitoTracker (C5 and D5; magenta in overlay images C4 and D4). Bassoon fragment Bsn9 (C1 and D1; magenta in overlay images C2 and D2) shows a uniform cytoplasmic distribution when coexpressed with Mito-EGFP control construct (C1–C3) but is corecruited to mitochondria when mito-targeted DLC1 is coexpressed (D1–D3). Bar, 10 µm.

A

```
hs NM_003458     YGQPPTTANYGSQTEELPHAPSGPPGSGRAPREKPLSGGDSEVGAPQPSR 1473
rn NM_019146     YGHSPTTANYGSQTEDLPQAPSGLAAAGRAAREKPLSASDGEGGTPQPSR 1468
mm NM_007567     YGQPPTTANYGSQTEELPHAPSGPAGSGRASREKPLSGGDGEVGPPQPSR 1461
oa XM_001521666 LGQAQIPAGYGSQTEEPPKPKSAADVGGTSAREKLQSLGDAKSGVPVSPK 958
gg XR_027062     YSPAKSTISYGSQTEDITRSKVGVETSVQTAREKLQAVSDGK---PPPAK 652
dr XR_029870     NVSHKIAAITQAYNQRESAARKMAISRGVQMRDSSTSSDTRIESGPSSIR 1595
                       .    : .:  . .           *:.  : .      * . :

hs NM_003458     AYSYFASSSPPLSPSSPSESPTFSPGKMGP------RATAEFSTQTPSPA 1512
rn NM_019146     GYSYFTGSSPPLSPSTPSESPTFSPSKLGP------RATAEFSTQTPSLT 1505
mm NM_007567     GYSYFTGSSPPLSPSTPSESPTFSPGKLGP------RATAEFSTQTPSLT 1517
oa XM_001521666 GYPYFKSSSPPLSPTSPTESPPHSAVRIGPGPG--LRSTVEFSTQTQSPM 1006
gg XR_027062     TYSFFKSSSPPLSPTSPTQSPTHAAPRAAAPSGPTAKSTAEFSTQTQSPL 702
dr XR_029870     SYAYHE-RSPPLSPTS---SPTHSPTRSPS------RRTAEFSTQTVSPS 1635
                  *.:.   ******::   **..:. :  .      : *.****** *

hs NM_003458     PASDMPRSPGAPTPSPMVAQGTQTPHRPSTPRLVWQESSQEAPFMVITLA 1562
rn NM_019146     PSSDIPRSPGT--PSPMVAQGTQTPHRPSTPRLVWQQSSQEAPVMVITLA 1553
mm NM_007567     LSSDIPRSPGP--PSPMVAQGTQTPHRPSTPRLVWQQSSQEAPIMVITLA 1565
oa XM_001521666 LSVDAPVGPGSSTASPMVAQGTQTPHRSSSPRLTRQQSSQDSPFMVITLA 1056
gg XR_027062     LAYDVPTTTGPSASSPMVAQGTQTPHRAGSPRLTRQQSSQDAPFMLITLA 752
dr XR_029870     ---VLASSGNASHTSPVMAQGTQTSHGVVTPGLFRQQSTQDTYYMIRTEE 1682
                      .   ..  .**::******.*   :* *  *:*:*::  *: *
```

B

| | DLC1 MBAx$10^{-3}$ mean ±SD | DLC2 MBAx$10^{-3}$ mean ±SD |
|---|---|---|
| Bsn 9 | 34.3±3.1 | 52.7±2.5 |
| Bsn $9^{II}$ | 19.3±1.2 | 17.7±3.5 |
| Bsn $9^{III}$ | 18.3±3.6 | 21.6±3.1 |
| Bsn $9^{II,III}$ | 6.3±0.6 | 6.7±1.2 |
| Bsn 12 | 50±7 | 44±5.3 |
| Bsn $12^{I}$ | 10.3±1.2 | 9.3±2.1 |
| Bsn 13 | 91.3±6.3 | 110.3±4 |
| Bsn $13^{I,II,III}$ | 1.7±0.6 | 2±0 |

Figure S3. **DLC-binding motifs of Bassoon.** (A) Conservation during vertebrate evolution. Alignment of amino acid sequences of human (hs), rat (rn), mouse (mm), platypus (oa), chicken (gg), and zebrafish (dr) Bassoon orthologues. The DLC-binding motifs are highlighted in gray. Note that the second and third motifs are completely conserved in all species displayed, whereas the first motif is not conserved in fish. Asterisks indicate identical residues, colons indicate conserved substitutions, and periods indicate semiconserved substitutions. (B) Results of surface plasmon resonance binding assays (Fig. 3 C). The molecular-binding activity (MBA) was calculated from three to five association–dissociation cycles performed for each interaction pair. The results shown were confirmed by a second measurement set in which proteins coming from independent purifications were used.

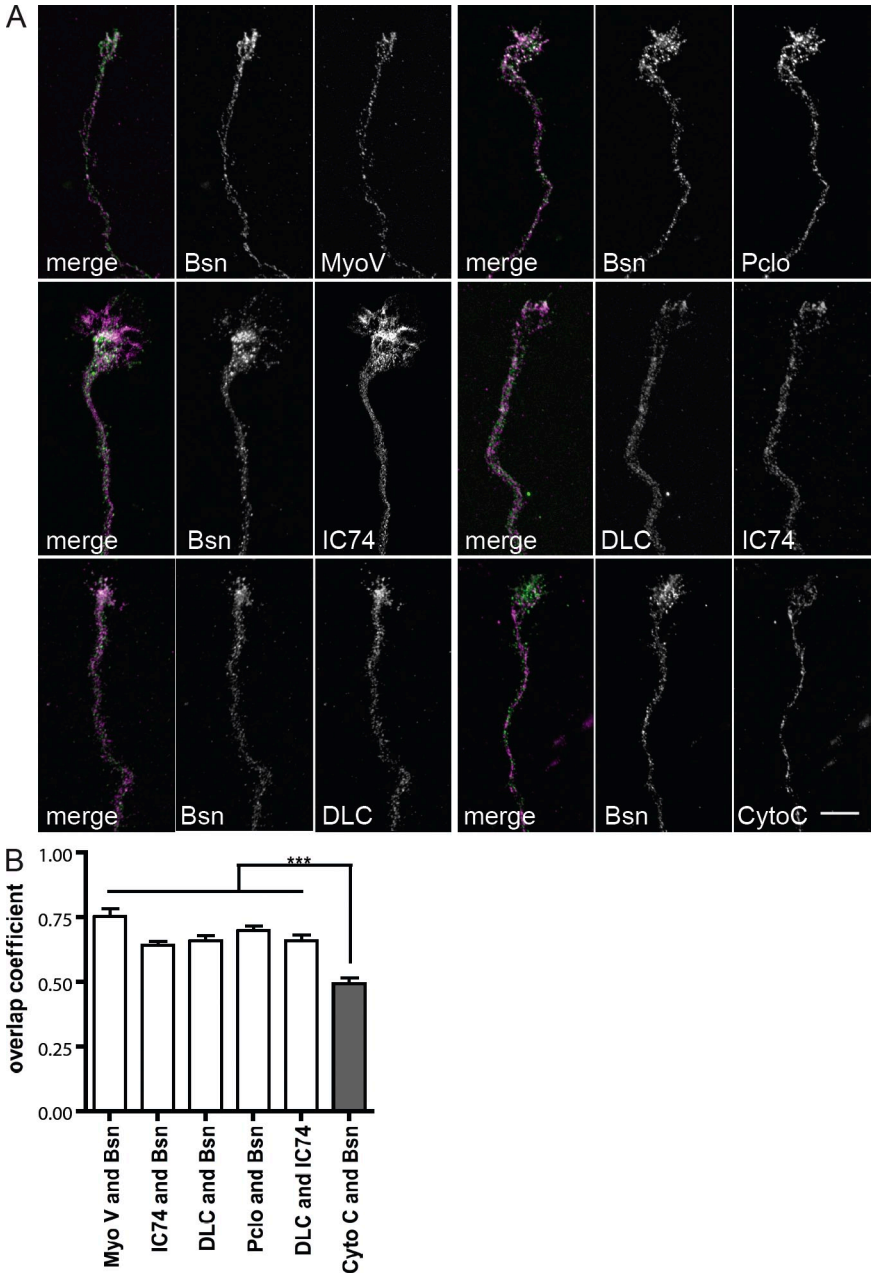


Figure S4. **Quantification of colocalization of Bassoon with myosin V, IC74, DLC8, Piccolo, and cytochrome *c* and of DLC8 with IC74 in distal axonal segments of 5 DIV neurons.** (A) Example images used for colocalization analysis are shown. (B) Bar graph of mean OC calculated from at least 10 independent images. Error bars indicate SEM; ***, $P < 0.001$ (one-way analysis of variance). Bsn, Bassoon; CytoC, cytochrome *c*; MyoV, myosin V; Pclo, Piccolo. Bar, 10 µm.

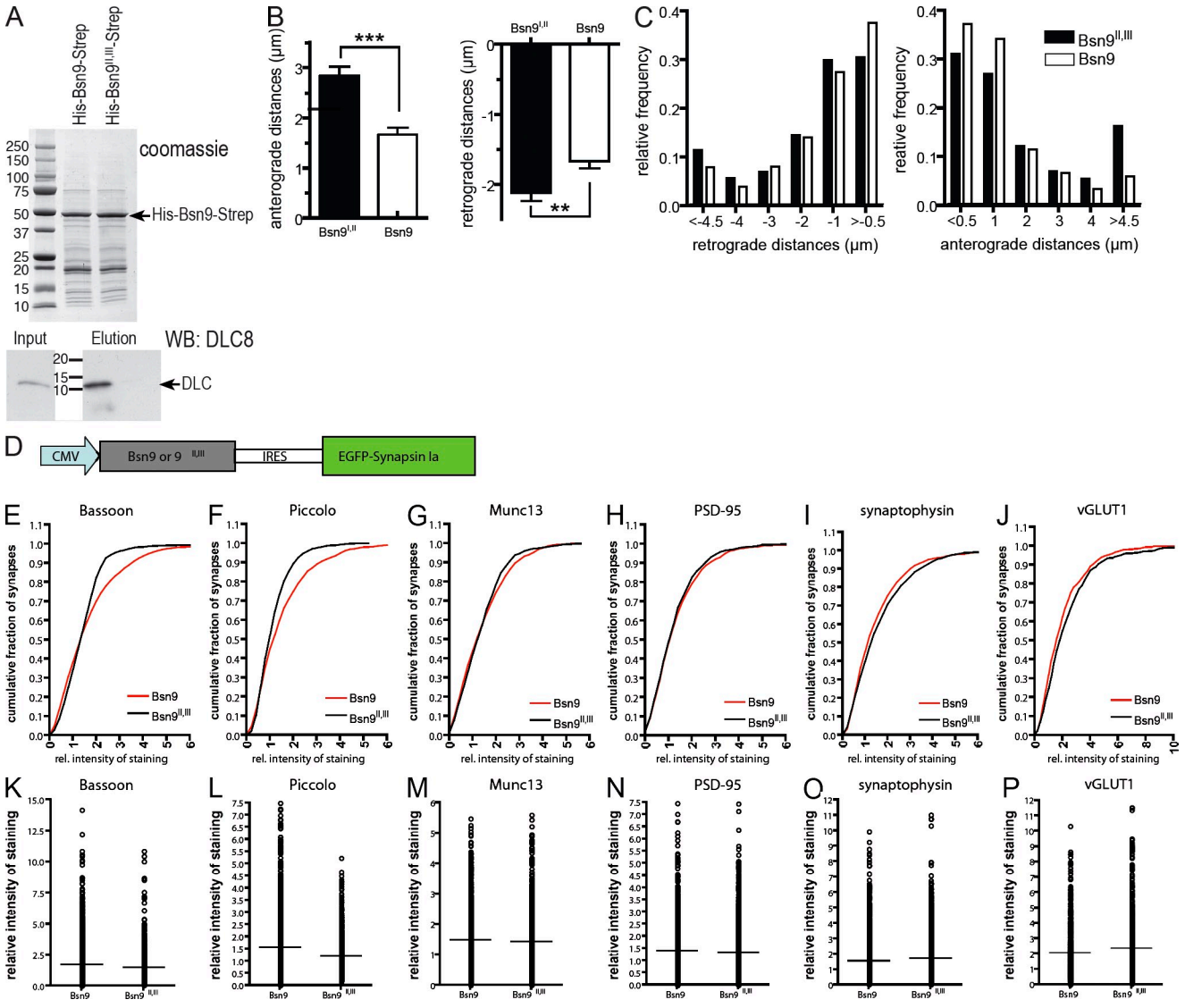


Figure S5. **Interference with Bassoon–DLC interaction in neurons.** (A) Pull-down experiment showing that endogenous DLC is efficiently captured by Bsn9 but not by Bsn9$^{II,III}$ (bearing point-mutated DLC-binding sites) from brain lysate. Molecular mass is indicated in kilodaltons. (B and C) The overexpression of Bsn9 affects GFP-Bsn trafficking in neurons. Running distances of movements in both directions were analyzed. (B) Bar graphs show mean values of running distances for GFP-Bsn with co-overexpressed Bsn9 (open bars) or Bsn9$^{II,III}$ (shaded bars). Error bars indicate SEM; **, P <0.01; ***, P < 0.001. (C) Relative distribution of analyzed running distances (significant difference: P, < 0.001 in two-way analysis of variance of cumulative frequency distribution of values). (D) Scheme illustrating the expression cassette used for interference with DLC–Bassoon interaction in a dominant-negative approach. Dominant-negative construct Bsn9 carrying two of Bassoon's DLC-binding sites or control construct Bsn$^{II,III}$ lacking these sites (see Fig. 3) was overexpressed in primary neurons transfected at 3 DIV and evaluated at 9 DIV. Synapses were labeled by coexpression of EGFP-synapsin from the same vector encoding a bicistronic transcript. CMV, promoter or cytomegalovirus; IRES, internal ribosomal entry site. (E–P) Intensities and variances for Bassoon (E and K), Piccolo (F and L), Munc13 (G and M), PSD-95 (H and N), synaptophysin (I and O), and vGLUT1 (J and P) at synapses were detected and normalized as described in Materials and methods. (E–J) Plots show the cumulative distribution of relative fluorescent intensities for respective stainings. Note the different distribution of Bassoon and Piccolo staining intensities in cells transfected with Bsn9 construct as compared with the control Bsn9$^{II,III}$. (K–P) Scatter plots show distribution of values of intensities of individual synapses. Of note, the mean staining intensities (E and F) and the variance of intensities at individual synapses (K and L) is increased for Bassoon and Piccolo but not for Munc13, PSD-95, or SV markers synaptophysin and vGLUT1.

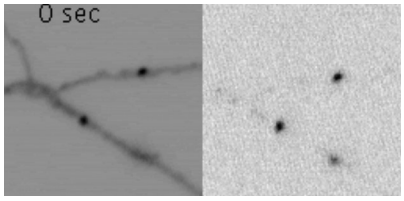


Video 1. **DLC1-EGFP co-migrates with mRFP-Bsn in neurons.** The video shows a section of an axonal tree of a neuron transfected with DLC1-EGFP and mRFP-Bsn at 3 DIV and analyzed 2 d later. Recording of DLC1-EGFP fluorescence is shown in the left part and mRFP-Bsn fluorescence in the right part of the combined image. Note the co-migration of mRFP-Bsn particles with DLC1-EGFP (compare with Fig. 4 A). The video is shown at 30 frames/s.

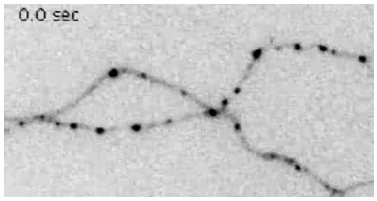


Video 2. **Mobility of GFP-Bsn in neurons.** The video shows a section of an axonal tree of a neuron transfected with the GFP-Bsn construct at 3 DIV. The video was recorded 48 h after transfection. Note the smaller, dimmer fluorescent particles that move faster and more directionally than the bigger, brighter particles, which show more restricted forward and backward movements. The video is shown at 90 frames/s.

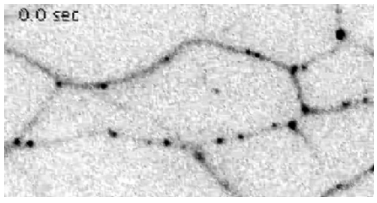


Video 3. **GFP-BsnDBM shows decreased mobility compared with GFP-Bsn in neurons.** The video shows a section of an axonal tree of a neuron transfected with the GFP-BsnDBM construct lacking all three DLC-binding sites at 3 DIV. The video was recorded 48 h after transfection. Note the striking difference in overall mobility of both smaller and bigger fluorescent particles as compared with Video 2. The video is shown at 90 frames/s.